Earth and Planetary Science Letters 469 (2017) 42–52

Contents lists available at ScienceDirect

Earth and Planetary Science Letters

www.elsevier.com/locate/epsl

The million-year evolution of the glacial trimline in the southernmost Ellsworth Mountains, Antarctica

David E. Sugden [a,*], Andrew S. Hein [a], John Woodward [b], Shasta M. Marrero [a], Ángel Rodés [c], Stuart A. Dunning [d], Finlay M. Stuart [c], Stewart P.H.T. Freeman [c], Kate Winter [b], Matthew J. Westoby [b]

[a] Institute of Geography, School of GeoSciences, University of Edinburgh, Edinburgh, EH8 9XP, UK
[b] Department of Geography, Northumbria University, Newcastle upon Tyne, NE1 8ST, UK
[c] Scottish Universities Environmental Research Centre, Rankine Avenue, East Kilbride, G75 0QF, UK
[d] School of Geography, Politics and Sociology, Newcastle University, Newcastle upon Tyne, NE1 7RU, UK

ARTICLE INFO

Article history:
Received 23 December 2016
Received in revised form 28 March 2017
Accepted 2 April 2017
Available online xxxx
Editor: A. Yin

Keywords:
West Antarctic Ice Sheet
Ellsworth Mountains
glacial trimline
exposure ages
mid-Miocene
depth profile

ABSTRACT

An elevated erosional trimline in the heart of West Antarctica in the Ellsworth Mountains tells of thicker ice in the past and represents an important yet ambiguous stage in the evolution of the Antarctic Ice Sheet. Here we analyse the geomorphology of massifs in the southernmost Heritage Range where the surfaces associated with the trimline are overlain by surficial deposits that have the potential to be dated through cosmogenic nuclide analysis. Analysis of 100 rock samples reveals that some clasts have been exposed on glacially moulded surfaces for 1.4 Ma and perhaps more than 3.5 Ma, while others reflect fluctuations in thickness during Quaternary glacial cycles. Modelling the age of the glacially moulded bedrock surface based on cosmogenic ^{10}Be, ^{26}Al and ^{21}Ne concentrations from a depth-profile indicates a minimum exposure age of 2.1–2.6 Ma. We conclude that the glacially eroded surfaces adjacent to the trimline predate the Last Glacial Maximum and indeed the Quaternary. Since erosion was by warm-based ice near an ice-sheet upper margin, we suggest it first occurred during the early glaciations of Antarctica before the stepped cooling of the mid-Miocene at ∼14 Ma. This was a time when the interior Antarctic continent had summers warm enough for tundra vegetation to grow and for mountain glaciers to consist of ice at the pressure melting point. During these milder conditions, and subsequently, erosion of glacial troughs is likely to have lowered the ice-sheet surface in relation to the mountains. This means that the range of orbitally induced cyclic fluctuations in ice thickness have progressively been confined to lower elevations.

© 2017 The Authors. Published by Elsevier B.V. This is an open access article under the CC BY license (http://creativecommons.org/licenses/by/4.0/).

1. Aim

The aim is to examine the geomorphology of the three most southerly mountain massifs in the Heritage Range, part of the Ellsworth Mountains in Antarctica. The mountains protrude through the Antarctic Ice Sheet and feature a glacial trimline reflecting thicker ice than at present. The advantage of the sites in the southern Heritage Range is that, unlike most locations in the higher parts of the Ellsworth Mountains, here the ice-scoured bedrock adjacent to the trimline is overlain by glacial deposits with the potential of constraining its age and evolution.

2. Background

The Ellsworth Mountains, discovered by Lincoln Ellsworth in 1935, form a rugged range 350 km long and 80 km wide on the landward boundary of the Filchner–Ronne Ice Shelf in the Weddell Sea embayment (Fig. 1). The range runs NNW–SSE and the eastward flowing Minnesota Glacier separates the Sentinel Range to the north from the Heritage Range in the south. The Sentinel Range rises abruptly above the ice sheet and on its western side is an escarpment leading to a succession of peaks exceeding 3500 m and including the highest mountain in Antarctica, Mount Vinson at 4897 m. The Heritage Range is lower with peaks below 2500 m. The topography is dominated by a blend of longitudinal mountain ridges separated by glacier-filled basins with ice overspilling from the main ice sheet dome to the west. The southernmost massifs

* Corresponding author.
E-mail address: David.Sugden@ed.ac.uk (D.E. Sugden).

http://dx.doi.org/10.1016/j.epsl.2017.04.006
0012-821X/© 2017 The Authors. Published by Elsevier B.V. This is an open access article under the CC BY license (http://creativecommons.org/licenses/by/4.0/).

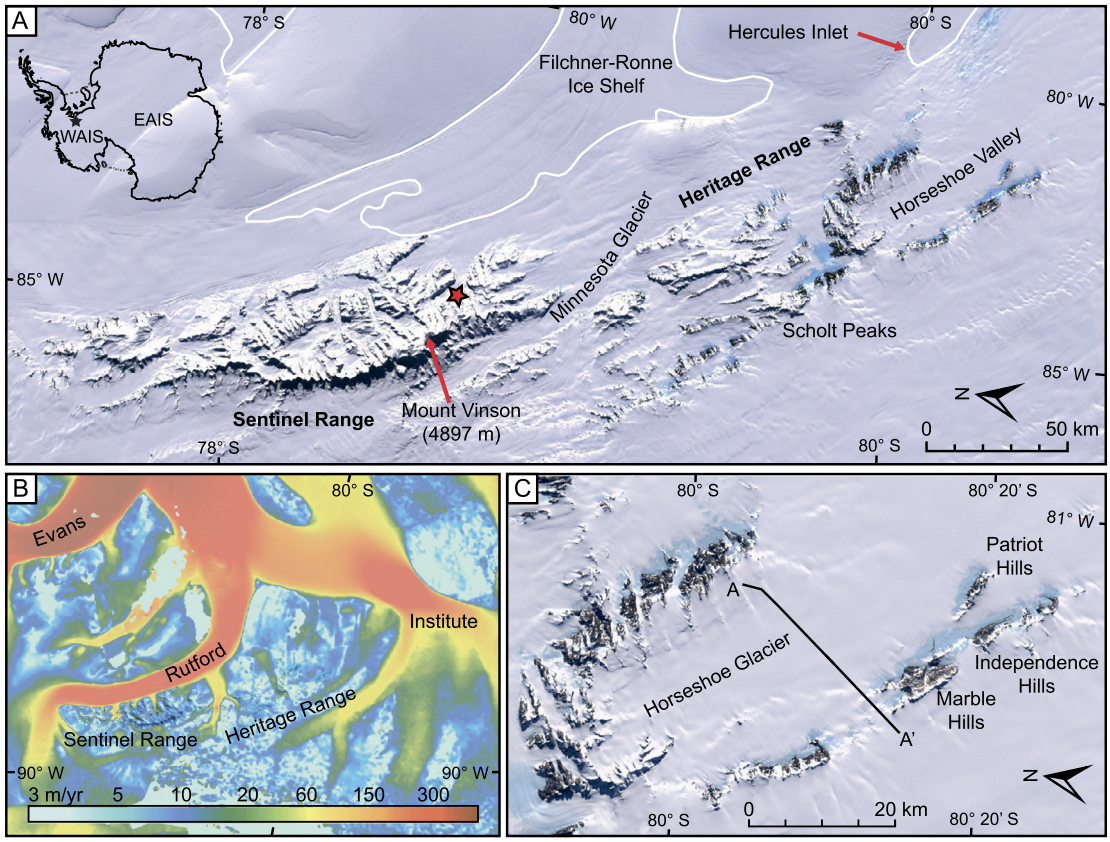

Fig. 1. (a) Moderate Resolution Imaging Spectroradiometer (MODIS) and Landsat Image Mosaic (LIMA) imagery of the Ellsworth Mountains showing the location of the Sentinel and Heritage ranges north and south of Minnesota Glacier and Mt. Vinson (4897 m), the highest peak in Antarctica. The location of the photograph in Fig. 2 is marked by a star. (b) Ice flow in the vicinity of the Ellsworth Mountains. The image shows satellite-derived surface ice flow velocities (m/yr) and the main ice streams (after Rignot et al., 2011). (c) The Marble, Patriot and Independence Hills and Horseshoe Glacier in their glaciological setting, showing the location of the radargram in Fig. 9.

of Marble Hills with the highest summit of Mt. Fordell (1670 m), Independence Hills with Mount Simmons (1590 m) and the Patriot Hills (1246 m), are surrounded by ice flowing into and along Horseshoe Glacier towards the southeast and east (Fig. 1c). The Heritage Range, unlike the Sentinel Range, experiences katabatic winds that sweep north-westwards across the main ridges and create blue-ice ablation areas on glaciers in their lee (Hein et al., 2016a). Upward glacier flow compensating for the surface ablation brings debris to the glacier surface and its margin. It is this latter process that explains the debris cover and marginal moraines of the mountain-foot glaciers of the southernmost massifs.

The Ellsworth Mountains consists of a conformable sequence of folded Cambrian to Permian sediments. Cambrian conglomerates and limestones are the dominant rocks of the Heritage Range, while younger quartzites underlie the high peaks of the Sentinel Range (Webers et al., 1992). The mountain block as a whole is thought to be a microplate that, prior to its separation around 140 million years ago, was part of what is now the East Antarctic continental plate (Storey et al., 1988; Fitzgerald and Stump, 1991). Glaciation is thought to have modified a pre-existing fluvial topography, the latter demonstrated by the dendritic pattern of valleys and the preservation of landscapes with rolling slopes around Mt. Vinson (Rutford, 1972). Many summits in the Sentinel Range and higher parts of the Heritage Range have been sculpted by alpine glaciers to form a landscape of horns, arêtes and sharp spurs (Denton et al., 1992).

A glacial trimline representing a higher elevation ice sheet has been described and mapped throughout the Ellsworth Mountains (Denton et al., 1992). It stands 400–650 m above the present ice sheet on the western side of the mountains and 1300–1900 m above the present surface of the Rutford Ice Stream to the east. The elevation of the trimline reflects the gradients of the present ice sheet surface and falls from the divide near the mid Sentinel Range towards the north, to the east towards the Weddell Sea, and to the south towards the Heritage Range (Fig. 1b). Denton et al. (1992) argued that this regionally consistent pattern shows that the trimline is an ice-marginal feature rather than an englacial thermal boundary. Although the latter possibility of a thermal boundary within the ice sheet has been used to explain an upper limit of glacial erosion beneath former ice sheets in the shield areas of northern mid-latitudes (Kleman et al., 1997), it would not explain the regionally consistent trimline elevation in the rough terrain of the Ellsworth Mountains. The trimline separates a glacially moulded and often striated bedrock surface from upper sharp mountain crests with fragile rock pinnacles (Fig. 2). The striations form two groups. One set of finely spaced, oxidised striations is associated with moulded and streamlined rock surfaces. These striations are typical of glacial abrasion beneath warm-based ice. Other striations that may cut through the oxidised set are discontinuous and irregular and typical of overriding cold-based ice. The age of the trimline and the glaciated surfaces beneath it have been controversial since its discovery. On the basis of the preservation of the striations and the nature of the drift, some have argued that the trimline represents the surface of a thicker West Antarctic Ice Sheet during the Last Glacial Maximum (LGM) (e.g. Rutford et al., 1980). Others have noted the great age of weathered striations in the Transantarctic Mountains and the difficulty of creating warm-based ice at the upper margin of an ice sheet during Antarctic climates of the last few million years (Denton et al., 1992). In this latter case the trimline could be millions of years old.

The contrasting views spill over into adjacent scientific fields. Early estimates of ice mass loss in West Antarctica based on the

Fig. 2. Striations and polish on roches moutonnées created by warm-based ice in a col underlain by quartzite on the eastern side of southern Sentinel Range (Fig. 1a). The col is close to the trimline and the serrated ridge in the background is above the trimline. Photo by George Denton.

Fig. 3. The drift-covered upland and valleys in the Marble Hills, showing the glacially moulded surface of the upland and Mount Fordell. All the peaks were inundated by warm-based ice at the time the highest trimline formed. Weathered erratics occur up to the base of Mount Fordell. The till patches are preferentially located in basins and on east facing slopes. The continuous dark-coloured till deposit in the middle distance is ice-cored.

Gravity Recovery and Climate Experiment (GRACE) satellite data, assumed a LGM age for the trimline, and thus postulated high estimates of subsequent ice-mass loss over the Ellsworth Mountains (Ivins and James, 2005). A review of field evidence for the LGM configuration of the quarter of the Antarctic Ice Sheet flowing into the Weddell Sea embayment suggested two contrasting reconstructions (Hillenbrand et al., 2014). One, compatible with a LGM age for the trimline, envisaged a thick ice sheet grounded as far as the offshore shelf edge with ice over 1000 m thicker in the Ellsworth Mountains. The alternative, based on cosmogenic nuclide dating, was for a thinner ice reconstruction in the Ellsworth Mountains (Bentley et al., 2010). If the trimline was LGM in age then it seemed to add support to the sea level community searching for the ice mass source for Meltwater Pulse 1A (Clark, 2011). There are also contrasting glaciological numerical models of the LGM. Golledge et al. (2013) lay weight on marine evidence of grounding offshore in the Weddell Sea and as a result model a thick LGM ice sheet with a surface altitude over 1000 m higher than the present ice surface near the Ellsworth Mountains. Alternatively, laying stress on low gradient ice streams, Le Brocq et al. (2011) modelled a thin ice sheet at the LGM with only a modest change in elevation near the Ellsworth Mountains. Clearly, knowing the age of the trimline and its associated glaciated surfaces would help constrain prevailing models.

3. The field area

The glaciated surfaces associated with the trimline are displayed in the Marble, Patriot and Independence Hills (Fig. 3). At the time of erosion, ice enveloped all the peaks in the field area and flowed towards Institute Ice Stream and thence to the Filchner–Ronne Ice Shelf (Denton et al., 1992) (Fig. 1b). Currently much of the ice flow into Horseshoe Glacier and the glacier itself is towards the grounding line at Hercules Inlet 45 km away.

The three mountain massifs consist of Cambrian limestones that outcrop in two facies: grey well-bedded limestones and white, massive marble-like limestones (Spörli and Craddock, 1992). The limestones are underlain by conglomerates that outcrop in the eastern Patriot Hills. The whole sequence has been folded and metamorphosed. Dark limestone characterises the Patriot Hills while white limestone dominates the higher peaks of the Marble and Independence hills. The erratics that occur on the massifs include many local limestones, but significantly they also include many exotic quartzites and basic igneous lithologies, the latter derived from the Scholt Peaks area some 70 km to the NNW (Denton et al., 1992).

4. Methods

Geomorphological mapping in the Patriot Hills was achieved by field examination of the main crest and the northern slopes of the massif. An embayment containing the largest concentration of blue-ice moraine was studied in detail (Westoby et al., 2016). In the Marble Hills mapping relied on remote sensing with selected field checks, including GPR. In the Independence Hills we concentrated on one altitudinal profile on an accessible spur and conducted several field and GPR surveys across the current blue-ice moraines. We sampled bedrock and erratic clasts for cosmogenic nuclide analysis. A depth profile was retrieved from sandstone bedrock on the eastern end of the Patriot Hills massif at a location ~120 m above the ice surface (Fig. 4). Here, a 5-cm diameter core was extracted using a portable backpack drill to a depth of 2 m, and cosmogenic ^{10}Be, ^{26}Al and ^{21}Ne were measured at six depths within the profile. For erratics, in order to minimise problems of inheritance and post-depositional movement, we sampled sub-rounded or sub-angular clasts with evidence of glacial abrasion such as striations. In the case of elevated clasts, we selected those that were resting firmly on bedrock. We also included samples emerging on the glacier surface in the blue-ice zone to test for possible inheritance. We have carried out ^{10}Be (99), ^{26}Al (63) and ^{21}Ne (23) analyses on 101 quartz-rich samples to determine exposure ages and possible long-term burial by ice. Full details of all ^{10}Be/^{26}Al/^{21}Ne are provided in Supplementary Tables 1–2. The samples were prepared in the Cosmogenic Nuclide Laboratory of the School of GeoSciences, University of Edinburgh, and measured at the AMS facility and noble gas laboratory at the Scottish Universities Environmental Research Centre (SUERC) using established procedures Hein et al. (2016a, 2016b). For exposure age calculations we used default settings in Version 2.0 of the CRONUS-calc programme and nuclide production rates from CRONUS-Earth (Marrero et al., 2016).

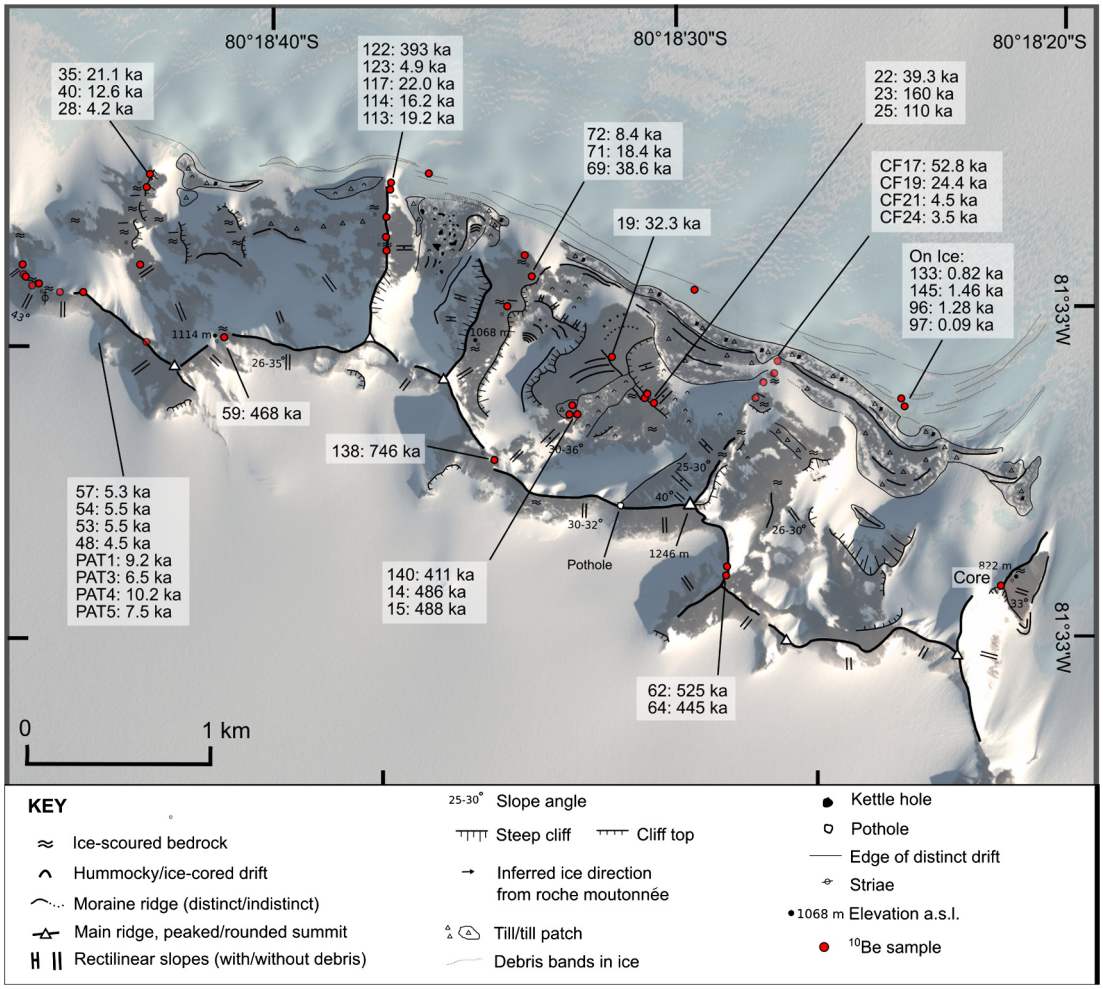

Fig. 4. Geomorphological map of the Patriot Hills showing main glacial landforms, the location and age of erratics sampled for ^{10}Be, and the bedrock core site. The roches moutonnées show ice flow across the spurs on the northeastern flank of the massif while ice-scouring occurs on parts of the crest. The oldest exposure ages occur on mountain crest erratics and on weathered till. The thinning signal from the last glaciation is best displayed on spurs in the northwest and on the north-facing spur between the two main blue-ice moraine embayments. The interplay between local debris-covered glaciers and Horseshoe Glacier leads to complex relationships.

5. Results: geomorphological observations

5.1. Patriot Hills

The Patriot Hills comprise a mountain crest some 8 km long with summits up to 1240 m that rise 750 m above the present surface of Horseshoe Glacier on the northern flank (Fig. 4). Horseshoe Glacier is 2250 m thick and flows eastwards in a trough extending below sea level (Winter et al., 2015); a blue-ice zone and accompanying moraine occur along the glacier margin at the foot of the Patriot Hills.

The mountain crest itself is clearly delimited. In places where the elevation exceeds 1200 m the ridge crest is less than 1 m wide and bounded by slopes of 36–40°. Elsewhere the crest is tens to hundreds of metres across. Rectilinear slopes with angles usually in the range of 26–35° extend from the crest to the surrounding ice surface and dominate the southern flanks of the massif. Similar rectilinear slopes also occur on the sides of many valleys that punctuate the northern flanks of Patriot Hills. Cliffs with sharp upper edges and slopes steeper than 45° occur on the northern side of the massif, especially on the lateral slopes of the main valleys supporting debris-covered glaciers. Smaller cliffs bound small glaciers perched on both the southern and northern flanks of the mountains. Landforms of glacial erosion formed by overriding ice are visible on the northern spurs. Here a succession of 10–100 m-long roches moutonnées display ice-moulded upper surfaces and cliffed east-facing borders; they are most common on the tops of the main spurs especially at lower elevations (Fig. 5a). In addition, ice moulded bedrock surfaces with joints and structures deepened up to a few metres and the intervening bumps smoothed on their west-facing sides occur on all spurs, in saddles, and in several locations on the mountain crestline up to an elevation of 1150 m. One final feature of interest on a saddle on the mountain crestline is a circular pothole, tens of metres across and ∼10 m deep, that is cliffed on its east-facing side (Fig. 5b).

The Patriot Hills display two sets of glacial deposit: exotic and local. The exotic deposits include current and past blue-ice moraines. The current blue-ice moraines have been analysed in detail (Westoby et al., 2016) and are formed by upward flow of ice bringing basal debris, some of it exotic, from the bottom of the surrounding glaciers (Hein et al., 2016a). At the foot of the mountain slope the unweathered clasts are mixed with slope debris. Higher up the slope, as far as 270 m above the present ice edge, unweathered erratics form concentrations or ridges parallel to the mountain front or, more commonly, occur as scattered erratics consisting mainly of sandstone and some basic igneous lithologies. Weathered exotic deposits occur in places on the mountain front as patches of oxidised and frost-shattered till (Fig. 5c). In many locations there are scattered weathered erratics, including some on the crestline at an elevation of 1190 m. All contain exotic rocks similar in lithology to the current unweathered blue-ice moraines.

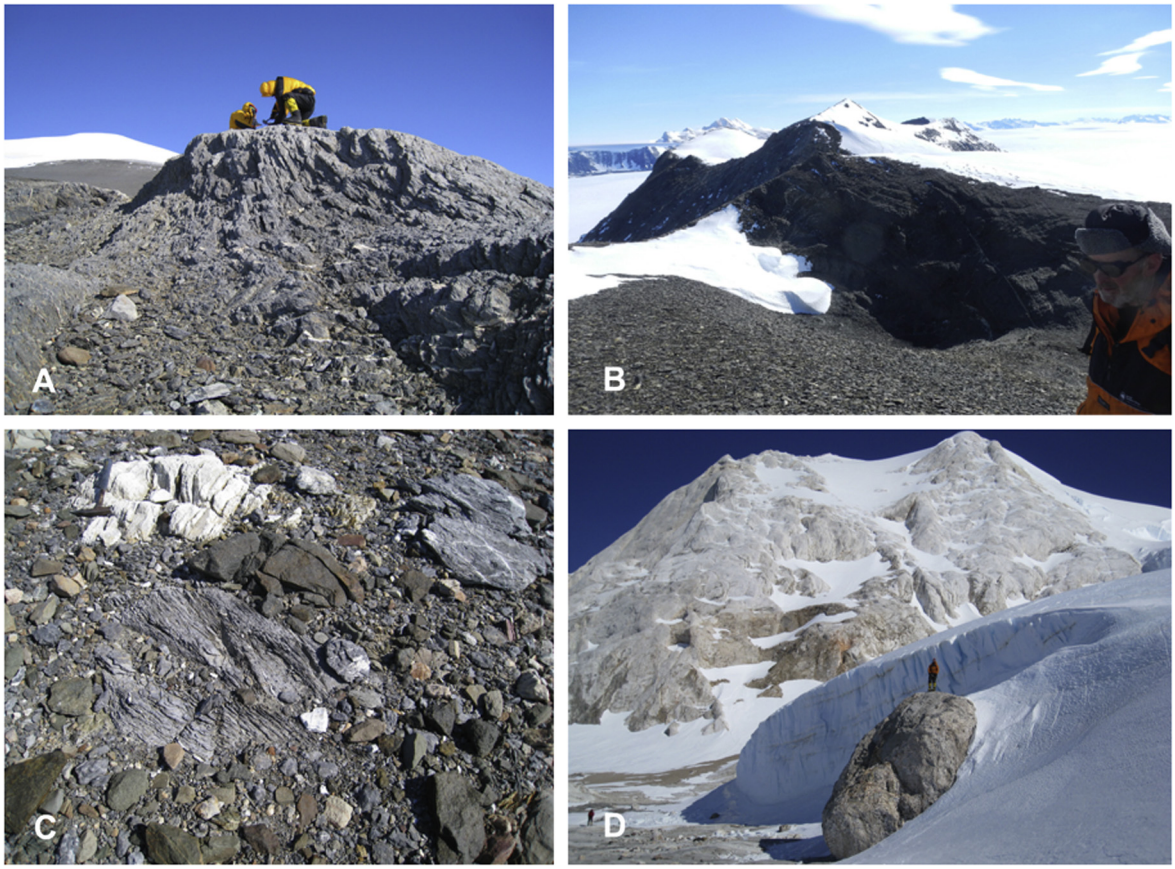

Fig. 5. (a) Photo of a roche moutonnée on a northern spur of the Patriot Hills. (b) The pothole on the crest of the Patriot Hills at ∼1200 m. (c) The frost shattered remnant of weathered till at an elevation of 1000 m in the Patriot Hills. Cosmogenic nuclide analysis points to a burial signal. Geological hammer for scale at upper left. (d) A large boulder of local limestone at the foot of Mt. Fordell's wind-drift glacier. The dark clasts are weathered exotic erratics with exposure ages at this altitude of ∼1.4 Ma.

A suite of landforms comprised wholly of local lithologies is associated with buried ice derived from local wind-drift glaciers. The two longest valleys support debris-covered/rock glaciers that have arcuate lineations indicating downslope flow. The south-easterly example is bounded by cliffs that provide a source of large limestone blocks that are intricately linked with both the current and elevated blue-ice moraines. The north-western example is covered with fine sedimentary rock fragments (tens of cm in diameter) and its surface is pockmarked with kettle holes. Former flow by other rock glaciers bearing local debris is indicated by arcuate and slumped moraines further to the northwest.

5.2. Marble Hills

The Marble Hills consist of a 12 km-long crestline with pyramidal peaks such as Mt. Fordell (1670 m), flanked to the southwest by ice from the main West Antarctic Ice Sheet dome at an elevation of 1400 m (Fig. 6). To the northeast of the crestline, and separated by a sharp break of slope, is a rolling upland 3–4 km across (Fig. 3). The upland is divided by two converging valleys that fall in elevation to a basin more than 200 m below the elevation of the main glacier. The surrounding upland consists of ice-scoured convex and concave slopes with many 10–100 m-long roche moutonnées with small cliffs on their eastern sides. Both the south-eastern and north-western edges of the massif are bounded by overspill glaciers from the ice dome that flow into Horseshoe Glacier. Local wind-drift glaciers form in the lee of the main mountain crestline. The edge of the upland overlooking Horseshoe Glacier at an elevation of 1100 m is cliffed in many places with the upper edge often rounded off. In places on the northern ridge of the upland, several gullies 10–100 m wide are cut across and down the eastern side of the ridge. These link with circular potholes tens of m across and of similar depth that are excavated into bedrock.

The Marble Hills also display two sets of glacial deposits: exotic and local. The current blue-ice moraine with mainly fresh exotic clasts fronts the base of the northern cliffs and, after a break, a continuation bends round towards Horseshoe Glacier as it merges with an overspill glacier to the east. The lithologies include quartzite, sandstone, shale, slate, limestone and basic igneous lithologies. Fresh clasts are scattered on bedrock up to an elevation 475 m above the ice surface where there are sheets of till and a moraine ridge on the western upland edge (Hein et al., 2016b). Some fresh till on the upland overlies buried, foliated glacier ice (Fig. 3). Weathered erratics and till are dominant at elevations above the fresh deposits, but also occur in patches at lower levels. The debris comprises a mix of mainly quartzite, sandstone and basic igneous clasts, all of which are oxidised and weathered. The range and nature of quartz-rich clasts in both current and elevated deposits is similar. However, more easily weathered shales, slates and limestones, common in the current and unweathered deposits, are rare in the weathered deposits. Local drifts are associated with wind-drift glaciers tucked in behind the main crestline; these comprise scattered boulders of local limestone, sometimes forming linear concentrations parallel to, but beyond the current glacier snout (Fig. 5d). In places, such latter concentrations lie among weathered exotic clasts.

5.3. Independence Hills

The Independence Hills form a 12 km-long mountain crest with several peaks over 1400 m. The ice sheet is at an elevation of 1200 m to the west while the ice surface to the east is around

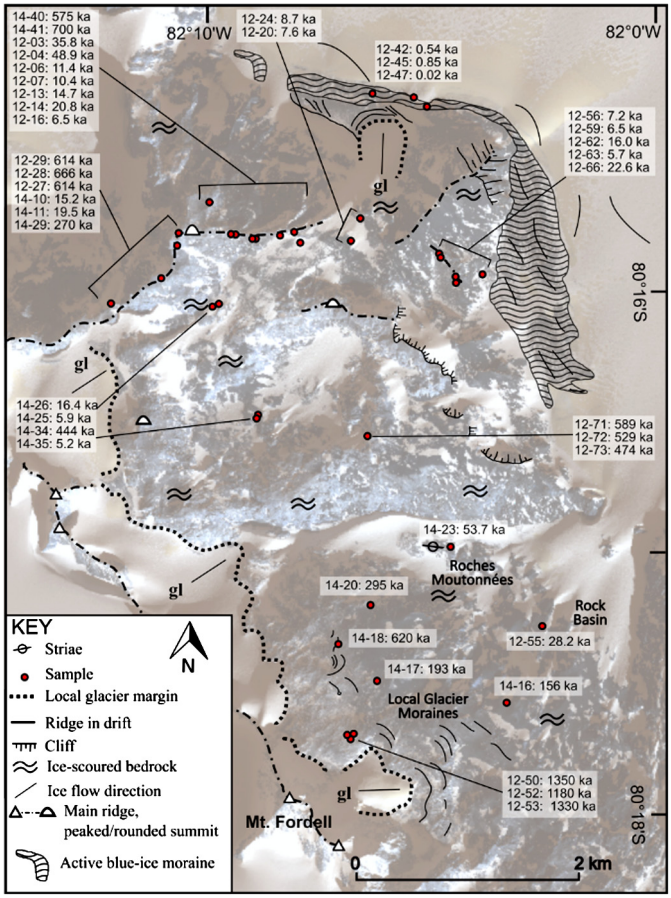

Fig. 6. The Marble Hills showing the main geomorphological features and the location and ^{10}Be ages of erratic samples. The oldest, highest weathered erratics with simple exposure occur at the foot of Mount Fordell and on the dome-shaped spur to the north. Lower, weathered erratics display a burial signal. The thinning signal from the last glaciation is best seen on the spurs to the north, but there is considerable scatter.

800 m. Our work focused on the blue-ice moraine and the steep lower slopes of the northern side of the mountains. This area comprises 200–600 m high cliffs with slopes commonly over 45°. The most impressive geomorphological feature is an 11 km-long blue ice moraine that sweeps eastwards from the mountain foot and is increasingly displaced from it by ice flowing down the mountain front (Fig. 7a). Elevated, fresh erratics are perched on cliffs and ridges overlooking the glacier. At elevations up to 400 m above the present glacier surface are patches of light brown till, 1–2 m thick, containing quartzite, sandstone, metamorphic slate, limestone, conglomerate and igneous lithologies (Fig. 7b).

5.4. Chronology

Cosmogenic nuclide analyses provide an insight into the glacial history of the three massifs. The weathered deposits yield exposure ages of 0.2–2.4 Ma, while the unweathered deposits, relating to the last glacial cycle, have ages of 3–49 ka (Figs. 4 and 6. Supplementary Tables 1–2). Boulders on the blue-ice glacier surface have ages of 0–1.5 ka, confirming their recent arrival at the surface by upward ice flow.

The oldest ^{21}Ne exposure age of an erratic on an ice-scoured bedrock surface on the crest of the Patriot Hills of 2.5 Ma has a ^{10}Be age of 0.75 Ma and ^{26}Al age of 0.56 Ma. The ^{26}Al/^{10}Be ratio requires 0.2–0.3 Ma of burial, while the ^{21}Ne/^{10}Be ratio indicates more than 1 Ma of burial (Supplementary Fig. S1). The difference between the ratios suggests that the erratic experienced a complex history of repeated burial during which the signal decayed, followed by intervals of exposure when it accumulated cosmogenic nuclides. Overall, the ^{21}Ne/^{10}Be ratio indicates that the erratic has a complex exposure-burial history amounting to at least 3.5 Ma. The erratic may have first been deposited on this ice-scoured surface before 3.5 Ma.

The analysis of the weathered deposits and their age relationships in the Marble Hills suggest blue-ice conditions for at least 1.4 Ma with lower deposits exhibiting burial beneath overriding ice in response to fluctuations in ice thickness during glacial cycles (Hein et al., 2016a). Further, the decline in ages and increasing burial signal with falling elevation is consistent with, but does not mandate, a long-term lowering of the ice surface. The unweathered deposits reflect deposition since the LGM at 49–10 ka. Thinning began around 10 ka and accelerated at 6.5–3.5 ka in response to the Holocene migration of the grounding line to Hercules Inlet (Hein et al., 2016b).

The results from the depth profile in bedrock reinforce the conclusions based on the older erratics. ^{21}Ne, ^{10}Be and ^{26}Al concentrations were analysed at six depths within the 2 m core. Fig. 8a

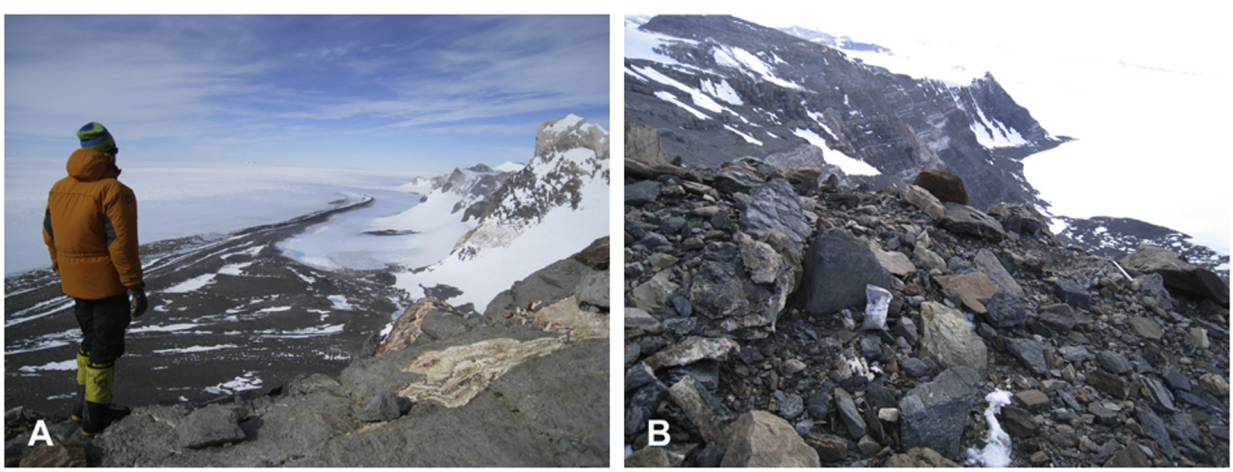

Fig. 7. (a) The view of the blue-ice moraine at the Independence Hills extending to the southeast. For most of its length, the moraine falls towards the east and is associated with uncrevassed ice surfaces. The moraine ridges, all of which are underlain by ice, form a complex pattern of linear and arcuate shapes. The linear features are adjacent to the main glacier and extend for kilometres; the arcuate features occur near the cliff. The highest ridge is adjacent to the main glacier and contains exotic, quartz-rich lithologies, especially sandstone. Moving towards the cliff there is a smaller ridge consisting wholly of upturned angular slate clasts, a small ridge of mixed exotic lithologies, a larger ridge of sandstone and limestone blocks and then another mixed deposit with gentle slopes that contains sandstone, siltstone and conglomerate. (b) A patch of weathered till comprising clasts and matrix at Independence Hills at ∼400 m above the glacier. Unweathered erratics also occur at the site.

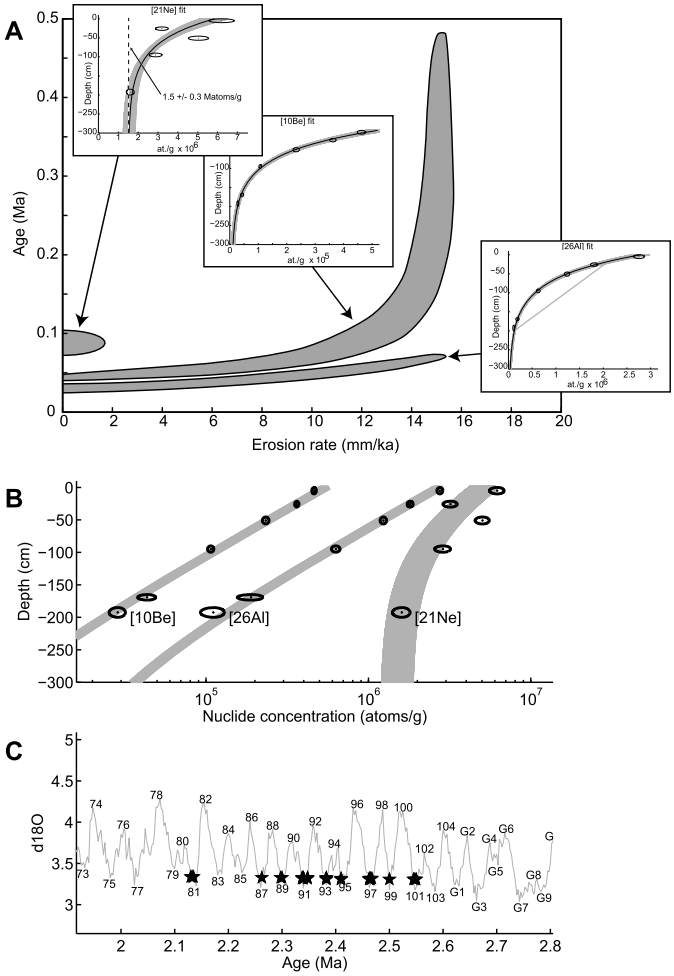

Fig. 8. Modelling of the bedrock depth profile following the approach of Rodés et al. (2011). (a) Plot showing the best model fits to each individual nuclide (inset plots) assuming constant exposure, and the incompatible relationships between age and erosion rate that result from making this assumption (1σ confidence limits). The modelling assumes constant exposure, rock densities between 2.55 and 2.65 g cm^{-3}, and no ^{10}Be or ^{26}Al inheritance. Models with inheritances of $1.5 \pm 0.3 \times 10^6$ atoms g^{-1} fit the ^{21}Ne dataset within 1σ. Results from the stable ^{21}Ne database indicate that the total exposure time of the surface is 89 ± 20 ka and the average erosion rate was <1.9 m/Ma during that time (1σ confidence limits). ^{10}Be and ^{26}Al production rates and corresponding attenuation lengths were calculated using Matlab code from online calculators formerly known as the CRONUS-Earth online calculators v. 2.3 (Balco et al., 2008) and a ^{21}Ne/^{10}Be production rate ratio of 4.1 was assumed for spallation and fast muons (Balco and Shuster, 2009). (b) The 52 model runs described below in (c) that fit the ^{21}Ne, ^{10}Be and ^{26}Al data within 1σ confidence limits. (c) The results of modelling an exposure-burial history marked by glacial cycles as represented by the LR04 isotopic marine record (Lisiecki and Raymo, 2005). The 52 model runs that are compatible with the measured ^{21}Ne, ^{10}Be and ^{26}Al concentrations (1σ) all lie between Marine Isotope Stages 81 and 101, corresponding to first exposure ages between 2.13 and 2.55 Ma. The model assumes that the surface is exposed during ice-free periods when the δ^{18}O is under a certain threshold, and is totally shielded from cosmic radiation during ice-covered periods when the δ^{18}O is above the considered threshold. The other parameter of the model is the age of the first exposure. The age-δ^{18}O space was calculated using the LR04 age spacing and every δ^{18}O = 0.005‰, which is less than the minimum δ^{18}O error in the LR04 dataset (0.02‰). As suggested by the best fits of the constant-exposure model to the ^{21}Ne dataset, no erosion and a ^{21}Ne inheritance of $1.5 \pm 0.3 times 10^6$ atoms g^{-1} are allowed. Results show a δ^{18}O threshold between 3.31 and 3.34‰, which is slightly higher than the current value of 3.23‰, and would be expected for a surface that is above the glacier surface today (see Supplementary Material and Supplementary Table S3 for further information).

models the best fitting exposure age and erosion rate for each individual nuclide assuming constant exposure since the bedrock was first exposed. The three nuclides reveal incompatible histories and thus show that the surface must have experienced a complex exposure-burial history. We then apply the Balco and Rovey (2008) method to test if the whole dataset is compatible with a single-cycle exposure-burial history. The linear fits show burial ages of 0.2 ± 0.2, 2.1 ± 0.7 and 1.2 ± 0.3 Ma for the ^{10}Be–^{26}Al, ^{21}Ne–^{10}Be and ^{21}Ne–^{26}Al isotope pairs, respectively. These discrepancies indicate a multi-cycle exposure-burial history. Using these data, we employ the global marine isotopic record of climate change collated by Lisiecki and Raymo (2005) as a basis for modelling an exposure-burial history that is compatible with the ^{21}Ne, ^{10}Be and ^{26}Al concentrations (Figs. 8b, 8c). We assume that the bedrock surface was exposed during ice-free periods when the marine δ^{18}O value is below a certain threshold, and totally shielded from cosmic radiation when the marine δ^{18}O value is above the threshold. This threshold and the age of first exposure are parameters in the model. The modelling shows that the optimum fit to the measured concentrations is achieved with a δ^{18}O threshold of 3.31 and 3.34‰, which is slightly higher than today's value of 3.23‰. The minimum age of first exposure is between 2.13 and 2.55 Ma (MIS 81–101). Including interglacial erosion as a third parameter in the model produces ages between 2.13 Ma and infinite, and erosion rates up to 10 m Ma^{-1}, but the model fit is not improved with respect to the no-erosion model. We recognise that there are uncertainties involved in relating Antarctic glaciations directly to the LR04 dataset, and yet random deviations from the record over 40 cycles will not have a major influence on the main conclusion that the bedrock was first exposed more than two million years ago.

It is interesting to note that the match improves if modest surface uplift relative to the glacier is incorporated. Surface uplift is simulated by increasing the δ^{18}O threshold over time. Models including moderate uplift rates fit the data better than those that consider no uplift. Optimum results reveal uplift rates of 0.14 δ^{18}O‰ Ma^{-1}, corresponding to first-exposure ages between 3 and 5 Ma. Thus, the ages between 2.13 and 2.55 Ma can be considered as minimum first-exposure ages.

6. Discussion

6.1. Interpretation of the geomorphology

The fact that only the tops of each massif protrude above the ice means that any record of landscape evolution is based on partial information. Nevertheless it is possible to reconstruct a record of landscape evolution from its earliest fluvial origins. The broad morphology of the three mountain massifs can be seen as reflecting a combination of tectonic and fluvial activity. The NNW–SSE orientation of the Marble and Independence Hills is conformable with the axes of folds and the exposure of rocks of differing resistance. On a more local scale the sinuous crestline of the Patriot Hills and Independence Hills is typical of a fluvial landscape where the crest adjusts through hillslope processes to the encroaching valley heads. Valleys flow away from the crestline in all three massifs. Straight slopes of 26–35° such as those on the southern flank of the Patriot Hills are commonly associated with sub-aerial erosion, especially in semi-arid environments (Summerfield, 1991). The escarpment incorporating Mt. Fordell displays a sharp break of slope at its foot as it meets the gently sloping upland of the Marble Hills. Radar surveys indicate a similar escarpment leading down to a subglacial plateau on the western side of the massif. Flattish surfaces and escarpments are characteristic of fluvial landscapes following rifting and result from accelerated erosion while the rivers adjust to the new base level (Kerr et al., 2000; Beaumont et al., 2000). In the McMurdo Dry Valleys, surfaces backed by escarpments have been attributed to fluvial incision following rifting ~60 million years ago, whilst a similar older topography exists in the Shackleton Range at the opposite end of the Transantarctic Mountains (Sugden et al., 1995, 2014). In the case

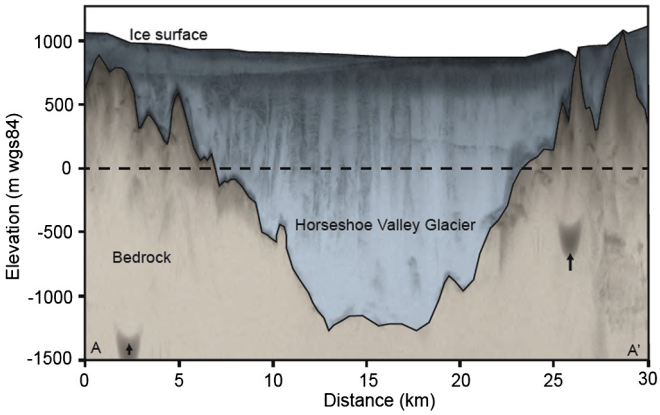

Fig. 9. Airborne radio echo sounding cross section of Horseshoe Valley trough. The radargram has been digitised to show the basal topography (brown), glacier ice (blue) and present-day sea level. The trough extends 1300 m below sea level. Arrows indicate processing artefacts. After Winter et al. (2015). (For interpretation of the references to colour in this figure legend, the reader is referred to the web version of this article.)

of the Heritage Range close to the edge of the Ellsworth Mountain block it is likely that a network of deep river valleys initially dissected the mountains following separation of the block from East Antarctica at ∼140 Ma. Fluvial erosion would be expected to erode plains near the coasts but maintain the mountain relief in response to isostatic uplift caused by erosion (Stern et al., 2005). It is this fluvial topography that would have experienced glaciation as Antarctica cooled in the Cenozoic, a conclusion that is in agreement with Rutford (1972) for the Sentinel Range.

The dominant signal of glacial modification is in the form of the deep troughs now located beneath Horseshoe Glacier and glaciers on either side of the Independence Hills. All three troughs are deepened beneath sea level; indeed Horseshoe Glacier extends 1300 m below present sea level (Fig. 9). Together these troughs indicate streaming flow of ice towards the southeast. A similar direction of flow is demonstrated by the landforms of each upland massif. This is shown by the roches moutonnées of the northern spurs of the Patriot Hills, the preferential distribution of weathered deposits in the protected lee-side eastern slopes on the upland of Marble Hills and the presence of erratic lithologies derived from 70 km to the northwest. Together these indicate regional flow broadly towards the east and southeast.

The presence of roche moutonnée forms on both the Patriot and Marble Hills shows that the ice was erosive. It agrees with the observations of Denton et al. (1992) in the Sentinel Range where roches moutonnées and striated surfaces occur close to the upper limit of the trimline (Fig. 2). The implication is that the ice was sliding at the ice-rock interface sufficiently to abrade the up-ice surface into a convex form and pluck rock from the lee side. These processes occur beneath warm-based ice and are rare beneath cold-based ice. Possible evidence of meltwater erosion comes from large potholes tens of metres across and ∼10 m deep associated with ridges and channels. The location of the potholes and channels near saddles is similar to the setting of subglacial meltwater channel systems at Battleship Promontory, Convoy Range in the McMurdo Dry Valley area (Sugden and Denton, 2004). Further study would be required to establish their origin unambiguously, but here we use it as additional evidence to suggest that meltwater was associated with glaciation of the trimline.

The climate that permitted warm-based ice to be present at an ice-sheet margin must have been markedly warmer than present. The Mean Annual Temperature (MAT) around the Ellsworth Mountains is currently estimated to be around −30 °C (Connolley and Cattle, 1994). This is in agreement with temperature measurements near the Patriot Hills, where firn at the relatively low altitude of 750 m and depth of 5 m was −26 °C in 1995 (Casassa et al., 2004). What change would be necessary to form warm-based ice? Use of a thermomechanically coupled glaciological model in the similar environment of the Olympus Range in the Transantarctic Mountains suggests that warm-based ice would require a MAT above −3 °C (Lewis et al., 2008); such a figure would imply a MAT at least 23 °C warmer than present. However, a more conservative figure is obtained if one takes the analogy of the Greenland ice sheet where surface meltwater can occur high on the ice sheet and yet penetrate to the base. The MAT at a site near the upper limit of surface melting at Kan_M at an altitude of 1270 m was −10.9 °C in 2015 (http://www.promice.dk). In this case, and taking a present Ellsworth temperature of −26 °C, the difference in MAT is some 15 °C warmer than present. These are approximate estimates based on simple assumptions, but they are sufficient to indicate that the warm-based striations at the upper levels of the trimline must represent glaciation in a climate significantly warmer than present.

6.2. Age of the trimline?

The presence of a weathered erratic with an exposure history of at least 3.5 Ma since deposition on an ice-scoured bedrock surface on the summit ridge of the Patriot Hills is important. Its significance is backed up by the minimum age of first exposure of glacially moulded bedrock at 2.1–2.6 Ma, and by the presence of a suite of weathered erratics on ice-scoured landforms on the upland of the Marble Hills where exposure ages range from 0.4–1.4 Ma. These represent minimum ages for erosion of the surfaces below the trimline but above the present ice surface. Thus we can conclude from the older ages that such erosion does not relate to exposure during any Pleistocene glacial cycle.

The trend of decreasing age and increasing burial history with falling elevation towards the current ice margin is consistent with, but does not demand, an ice margin that has fluctuated in thickness but on a trajectory of overall decline. Hein et al. (2016a) have argued that the fluctuations in ice thickness reflect Pleistocene glacial cycles, in which low glacial sea levels cause the grounding line to migrate seawards; such migration would thicken ice close to the present day margin. They also suggested that an overall declining trend in ice elevation over millions of years is the result of the main glaciers, such as Horseshoe Glacier, deepening their troughs. Remote sensing has identified the presence of basal water beneath such glaciers and a clear example is the presence of Lake Ellsworth that occupies a trough west of the Ellsworth Mountains (Ross et al., 2014). Further, striated clasts emerging at the glacier surface in blue-ice areas suggest that warm-based ice exists at the bottom of such glaciers and is erosive. Looking further afield, it is tempting to suggest that the anomalously high elevation of the trimline in the Ellsworth Mountains bordering the Rutford Ice Stream is the result of erosion of an unusually large trough beneath the latter glacier and the consequent lowering of the ice surface relative to the mountains. In support of such an idea, observations have revealed dynamic land-forming processes beneath the glacier (King et al., 2016).

Striations, roches moutonnées and meltwater features indicate warm-based ice near the thin margin of the ice sheet at the time it moulded the trimline. When could this have occurred? It seems necessary to go back to the mid-Miocene to find an appropriately warm climate. At such a time $^{40}Ar/^{39}Ar$ volcanic ash dates show that mountain glaciers in the Transantarctic Mountains, specifically in the Olympus Range, were warm-based and depositing striated clasts and meltwater deposits (Lewis et al., 2007). Plant fossils associated with the glacial deposits suggest that mean summer temperatures were 5–7 °C, which is 17–19 °C warmer than at present (Lewis et al., 2008). A similarly aged association of warm-based glacial deposits and interbedded horizons containing plants

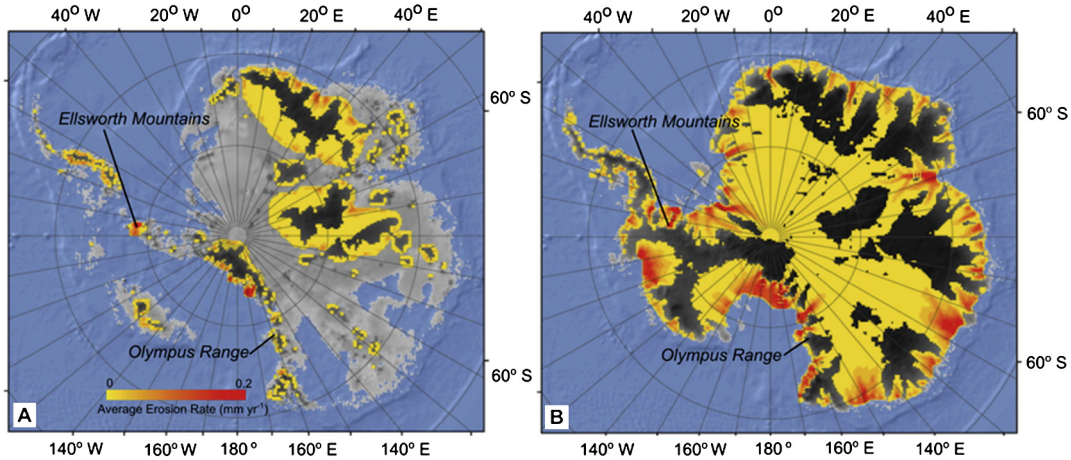

Fig. 10. The Antarctic ice sheet in a cooled Patagonian climate, typical of that in Antarctica during the early to middle Miocene, reveals ice at the pressure melting point in the Ellsworth Mountains. (a) Simulation with Antarctic sea-level temperature (MAT) at 2.4 °C. (b) The simulation with a sea-level temperature of −15 °C. The full ice sheet first forms when sea-level temperatures fall below −12 °C. The model shows rates of erosion that are related both to the occurrence of basal ice at the pressure melting point and to ice velocity. Yellow and red shading indicate areas with basal ice at the pressure melting point; within these areas, the difference in erosion rate relates to changes in ice velocity. Dark shading represents basal ice below the pressure melting point. (After Jamieson et al., 2010.) (For interpretation of the references to colour in this figure legend, the reader is referred to the web version of this article.)

and insects occurs at 1731 m on the flanks of Beardmore outlet glacier, only 550 km from the South Pole (Ashworth and Cantrill, 2004). Here there is a record of a tundra ground beetle, whose very close relative is found only in Tasmania (Ashworth and Erwin, 2016). Again this points to a summer climate several tens of degrees above that of today. This terrestrial evidence of warmer climatic conditions correlates with the mid-Miocene climatic optimum, identified in ocean sediment cores in the Ross Sea embayment (Warny et al., 2009). Thus, it seems that the Transantarctic Mountains at such a time must have supported warm-based mountain corrie glaciers and outlet glaciers that terminated in tundra vegetation within 550 km of the South Pole. It is likely that the Ellsworth Mountain block experienced a similar climate with mountain glaciers near the summits and ice-sheets extending over the main upland plateaux. The ice would have been warm-based and capable of eroding.

An insight into the nature of such a warm-based glaciation has been modelled by Jamieson et al. (2010). Recognising the similarity of vegetation in Oligocene deposits in Antarctica with that of Patagonia, the model simulates the glaciation of Antarctica by ramping down the climate from that of Patagonia (sea-level MAT of ∼6 °C) to that of present-day Antarctica (sea-level MAT of ∼−15 °C). At each step the ice sheet is allowed to reach equilibrium and the ice temperatures are calculated. There are many simplifications in the model but it does attempt to link ice extent with climate. Fig. 10a shows an early stage of ice-sheet growth with erosive warm-based ice in both the Ellsworth and Transantarctic Mountains. Fig. 10b shows a full Antarctic ice sheet first achieved when sea-level temperatures fall below −12 °C. At such a stage the basal ice is at the pressure melting point over wide peripheral areas of Antarctica, including the Ellsworth Mountains. The geometry of the ice sheet is similar to that of today and also that of the ice that moulded the elevated surfaces. Thus we suggest that the mid-Miocene ice sheet was capable of creating the glacial trimline and its associated surfaces.

It could be argued that a subsequent warm period, such as the Pliocene, with peak warmth at ∼3.1 Ma, could have seen widespread warm-based ice. This cannot be ruled out in view of evidence of fluctuations of the Ross Ice Shelf (Naish et al., 2009) and the suggestion that the East Antarctic Ice Sheet could have retreated from low-lying basins in the Pliocene (Scherer et al., 2016). However, there is evidence that the stepped cooling event at ∼14 Ma in the mid-Miocene was sufficient to drive Antarctica into its present dry polar regime with thin and local mountain glaciers becoming permanently cold-based. In the Olympus Range, the change from warm-based to cold-based till deposits is marked by an interbedded volcanic ash layer dated by $^{40}Ar/^{39}Ar$ at 13.89 Ma (Lewis et al., 2007). The biological evidence, dated independently by volcanic ash, suggests a fall in mean summer temperature of 17 °C (Lewis et al., 2008). Moreover, temperatures never recovered and constant dry polar conditions are indicated by the lack of meltwater activity and preservation of both unweathered volcanic ash and exquisitely preserved plant fossils. In Beacon Valley in the adjacent Quartermain Mountains, buried ice >8 Ma in age has survived beneath only 60 cm of rock debris (Marchant et al., 2002). These terrestrial fixes on a mid-Miocene cooling step in the history of the Antarctic Ice Sheet are mirrored in offshore records. Cores immediately offshore of the McMurdo Dry Valleys reveal cycles of ice sheet fluctuations with evidence of meltwater deposits until the mid-Miocene, after which the minimal volume of sedimentation points to unbroken polar conditions (Barrett, 2001; Naish et al., 2001). Deep sea ocean cores reveal a major stepped cooling of 6–7 °C at 14 Ma that was associated with the growth offshore of an expanded Antarctic Ice Sheet (Shevenell et al., 2004).

The coincidence of several independent sources of terrestrial evidence and marine records suggests that the whole of the Antarctic domain underwent stepped cooling in the mid-Miocene. It seems reasonable to suggest that the last time the Antarctic experienced sufficiently warm conditions to allow meltwater to exist beneath the upper margins of a coherent West Antarctic Ice Sheet was also ∼14 Ma ago. If so, then the main phase of erosion associated with the trimline in the Ellsworth Mountains occurred during or earlier than the mid-Miocene. Indeed, it could represent the full expansion of the ice sheet to the edge of the continental shelf in the Weddell Sea during which much of the Rutford trough and the deep Thiel trough beneath the Filchner–Ronne Ice Shelf were initiated. Such a Miocene expansion is inferred by an increase in exotic clasts in ocean sediment cores in the northern Weddell Sea (Anderson et al., 2011). In such a case the troughs and associated expansion are analogous to the troughs in the Dry Valleys where infill marine sediments demonstrate the troughs were cut by the mid-Miocene (Hall et al., 1993). The weathered and striated quartzite surfaces in the Ellsworth Mountains would have much in common with similarly old weathered and striated surfaces in the McMurdo Dry Valleys and mountainous Victoria Land (Orombelli et al., 1990). The presence of fresh but irregular and discontinu-

ous striations in the Sentinel Range suggests that surfaces near the trimline have been covered at some later stage(s) by cold-based ice. The paucity of striations in the Patriot, Marble and Independence massifs likely reflects weathering of less resistant limestones over millions of years.

If the trimline is so old, why are the deposits so much younger? One possibility is that we have not yet found the oldest erratics; another is that the erratics have eroded away. Yet another possibility is that they have only formed since blue ice areas were large enough to bring subglacial debris to the surface. This in turn requires mountain crests in an area of persistent katabatic winds to emerge sufficiently above the ice surface to create blue ice in their lee. If the million-year trajectory of the ice sheet is lowering in relation to the mountains due to erosion of surrounding troughs, then it might be that the southernmost massifs of the Heritage Range only emerged from beneath the ice sheet in the last few million years. The better match achieved by including relative uplift in the modelling of the depth-profile data is supportive of such a view.

7. Conclusion

This paper has examined three massifs in the southernmost Heritage Range in order to help date the Ellsworth glacial trimline, a feature representing a significant thickening and expansion of the West Antarctic Ice Sheet. Coupling detailed geomorphological analysis with an intensive campaign of cosmogenic nuclide exposure age dating, we show that glacial erosion of surfaces associated with the trimline is not of LGM or indeed Pleistocene age. The lower parts were covered by ice during the LGM, but the effect, in common with all Pleistocene fluctuations, was to add and redistribute blue-ice morainic debris onto an already eroded bedrock surface. Exposure age dating demonstrates that the surfaces adjacent to the trimline were sculpted more than two million years ago. Landforms indicating the presence of warm-based ice and meltwater at the edge of a large ice sheet require a climate similar to present-day Greenland where surface melting occurs at least seasonally. We argue that in Antarctica this last occurred in the mid-Miocene ∼14 million years ago. During the middle Miocene and subsequently, glacial erosion has lowered the glaciers in relation to the mountains by deepening surrounding troughs.

Author contributions

DES, ASH and JW conceived the project and carried out the fieldwork and analysis with SAD, SMM, KW and MJW. The cosmogenic analysis was by ASH, SPHTF, FMS, SMM and AR. All authors contributed to the writing of the paper and have approved the final version of this manuscript.

Acknowledgements

The research was supported by the UK Natural Environment Research Council: Grant numbers NE/1025840/1, NE/1034194/1 and NE/G013071/1. We thank the British Antarctic Survey for logistical and field support. Peter Nienow, Greg Balco and Johan Kleman added constructive insights.

Appendix A. Supplementary material

Supplementary material related to this article can be found online at http://dx.doi.org/10.1016/j.epsl.2017.04.006.

References

Anderson, J.B., Warny, S., Askin, R.A., Wellner, J.S., Bohaty, S.M., Kirshner, A.E., Livsey, D.N., Simms, A.R., Smith, T.R., Erhmann, W., Lawver, L.A., Barbeau, D., Wise, S.W., Kulhanek, D.K., Weaver, F.M., Majewski, W., 2011. Progessive Cenozoic cooling and the demise of Antarctica's last refugium. Proc. Natl. Acad. Sci. USA 108 (28), 11356–11360.

Ashworth, A.C., Cantrill, D.J., 2004. Neogene vegetation of the Meyer desert formation (Sirius Group) Transantarctic Mountains, Antarctica. Palaeogeogr. Palaeoclimatol. Palaeoecol. 213 (1–2), 65–82.

Ashworth, A.C., Erwin, T.L., 2016. *Antarctotrechus balli* sp.n. (Carabidae:Trechini): the first ground beetle from Antarctica. Zookeys 635, 109–122. http://dx.doi.org/10.3897/zookeys.635.10535.

Balco, G., Rovey, C.W., 2008. An isochron method for cosmogenic-nuclide dating of buried soils and sediments. Am. J. Sci. 308, 1083–1114. http://dx.doi.org/10.2475/10.2008.02.

Balco, G., Shuster, D.L., 2009. Production rate of cosmogenic ^{21}Ne in quartz estimated from ^{10}Be, ^{26}Al and ^{21}Ne concentrations in slowly eroding Antarctic bedrock surfaces. Earth Planet. Sci. Lett. 281, 48–58. http://dx.doi.org/10.1016/j.epsl.2009.02.006.

Balco, G., Stone, J.O., Lifton, N.A., Dunai, T.J., 2008. A complete and easily accessible means of calculating surface exposure ages or erosion rates from ^{10}Be and ^{26}Al measurements. Quat. Geochronol. 3, 174–195. http://dx.doi.org/10.1016/j.quageo.2007.12.001.

Barrett, P.J., 2001. Climate change – an Antarctic perspective. N.Z. Sci. Rev. 58, 18–23.

Beaumont, C., Kooi, H., Willett, S., 2000. Coupled tectonic-surface process models with applications to rifted margins and collisional orogens. In: Summerfield, M.A. (Ed.), Geomorphology and Global Tectonics. John Wiley and Sons, pp. 29–55.

Bentley, M.J., Fogwill, C.J., Le Brocq, A.M., Hubbard, A.L., Sugden, D.E., Dunai, T.J., Freeman, S., 2010. Deglacial history of the West Antarctic ice sheet in the Weddell Sea embayment: constraints on past ice volume change. Geology 38, 411–414.

Casassa, G., Rivera, A., Acuña, C., Brecher, H., Lange, H., 2004. Elevation change and ice flow at Horseshoe Valley, Patriot Hills, West Antarctica. Ann. Glaciol. 39 (1), 20–28. http://dx.doi.org/10.3189/172756404781814564.

Clark, P.U., 2011. Deglacial history of the West Antarctic ice sheet in the Weddell Sea embayment: constraints on past ice volume change: reply. Geology 39 (5), 239. http://dx.doi.org/10.1130/G31533C.1.

Connolley, W.M., Cattle, H., 1994. The Antarctic climate of the UKMO unified model. Antarct. Sci. 6, 115–122.

Denton, G.H., Bockheim, J.G., Rutford, R.H., Andersen, B.G., 1992. Glacial history of the Ellsworth Mountains, West Antarctica. Geol. Soc. Amer. Mem. 170, 403–432.

Fitzgerald, P.G., Stump, E., 1991. Early Cretaceous uplift in the Ellsworth Mountains of West Antarctica. Science 254 (5028), 92–94.

Golledge, N.R., Levy, R.H., McKay, R.M., Fogwill, C.J., White, D.A., Graham, A.G.C., Smith, J.A., Hillenbrand, C-D., Licht, K.J., Denton, G.H., Ackert, R.P., Maas, S.M., Hall, B.L., 2013. Glaciology and geological signature of the Last Glacial Maximum Antarctic ice sheet. Quat. Sci. Rev. 78, 225–247.

Hall, B.L., Denton, G.H., Lux, D.R., Bockheim, J.G., 1993. Late Tertiary paleoclimate and ice-sheet dynamics inferred from surficial deposits in Wright Valley. Geogr. Ann. Stockh. 75A, 239–267.

Hein, A.S., Woodward, J., Marrero, S.M., Dunning, S.A., Steig, E.J., Freeman, S.P.H.T., Stuart, F.M., Winter, K., Westoby, M.J., Sugden, D.E., 2016a. Evidence for the stability of the West Antarctic ice sheet divide for 1.4 million years. Nat. Commun. 7, 10325. http://dx.doi.org/10.1038/ncomms10325. 8 pp.

Hein, A.S., Woodward, J., Marrero, S.M., Dunning, S.A., Winter, K., Westoby, M.J., Freeman, S.P.H.T., Sugden, D.E., 2016b. Mid-Holocene pulse of thinning in the Weddell Sea sector of the West Antarctic ice sheet. Nat. Commun. 7, 12511. http://dx.doi.org/10.1038/ncomms12511. 8 pp.

Hillenbrand, C-D., Bentley, M.J., Stolldorf, T.G., Hein, A.S., Kuhn, G., Graham, A.G.C., Fogwill, C.J., Kristofferson, Y., Smith, J.A., Anderson, J.B., Larter, R.D., Melles, M., Hodgson, D.A., Mulvaney, R., Sugden, D.E., 2014. Reconstruction of changes in the Weddell Sea sector of the Antarctic ice sheet since the last glacial maximum. Quat. Sci. Rev. 100, 111–136.

Ivins, E.R., James, T.S., 2005. Antarctic glacial isostatic adjustment: a new assessment. Antarct. Sci. 17, 541–553.

Jamieson, S.S.R., Sugden, D.E., Hulton, N.R.J., 2010. The evolution of the subglacial landscape of Antarctica. Earth Planet. Sci. Lett. 293, 1–27. http://dx.doi.org/10.1016/j.epsl.2010.02.012.

Kerr, A., Sugden, D.E., Summerfield, M.A., 2000. Linking tectonics and landscape development in a passive margin setting: the Transantarctic Mountains. In: Summerfield, M.A. (Ed.), Geomorphology and Global Tectonics. John Wiley and Sons, pp. 303–319.

King, E.C., Pritchard, H.D., Smith, A.M., 2016. Subglacial landforms beneath Rutford Ice Stream, Antarctica: detailed bed topography from ice-penetrating radar. Earth Syst. Sci. Data 8, 151–158. http://dx.doi.org/10.5194/essd-8-151-2016.

Kleman, J., Hättestrand, C., Borgström, I., Stroeven, A., 1997. Fennoscandian palaeoglaciology reconstructed using a glacial geological inversion model. J. Glaciol. 43 (144), 283–299.

Le Brocq, A.M., Bentley, M.J., Hubbard, A., Fogwill, C.J., Sugden, D.E., Whitehouse, P.L., 2011. Reconstructing the Last Glacial Maximum ice sheet in the Weddell Sea embayment, Antarctica, using numerical modelling constrained by field evidence. Quat. Sci. Rev. 30, 2422–2432.

Lewis, A.R., Marchant, D.R., Ashworth, A.C., Hemming, S.R., Machlus, M.L., 2007. Major middle Miocene climate change: evidence from East Antarctica and the Transantarctic Mountains. Geol. Soc. Am. Bull. 119 (11–12), 1449–1461.

Lewis, A.R., Marchant, D.R., Ashworth, A.C., Hedenäs, L., Hemming, S.R., Johnson, J.V., Leng, M.J., Machlus, M.L., Newton, A.E., Raine, J.I., Willenbring, J.K., Williams, M., Wolfe, A.P., 2008. Mid-Miocene cooling and the extinction of tundra in continental Antarctica. Proc. Natl. Acad. Sci. USA 105 (31), 10676–10680.

Lisiecki, L., Raymo, M.E., 2005. A Pliocene-Pleistocene stack of 57 globally distributed benthic δ^{18}O records. Paleoceanography 20, PA 1003. http://dx.doi.org/10.1029/2004PA001071.

Marchant, D.R., Lewis, A.R., Phillips, W.M., Moore, E.J., Souchez, R.A., Denton, G.H., Sugden, D.E., Potter, N., Landis, G.P., 2002. Formation of patterned ground and sublimation till over Miocene glacier ice in Beacon Valley, southern Victoria Land, Antarctica. Geol. Soc. Am. Bull. 114 (6), 718–730.

Marrero, S.M., et al., 2016. Cosmogenic nuclide systematics and the CRONUScalc program. Quat. Geochronol. 31, 160–187.

Naish, T.R., Woolfe, K.J., Barrett, P.J., Wilson, G.S., Atkins, C., Bohaty, S.M., Bucker, C., Claps, M., Davey, F., Dunbar, G., Dunn, A., Fielding, C.R., Florindo, F., Hannah, M., Harwood, D.M., Watkins, D., Henrys, S., Krisseck, L., Lavelle, M., van der Meer, J.J.P., McIntosh, M.C., Niessen, F., Passchier, S., Powell, R., Roberts, A.P., Sagnotti, L., Scherer, R.P., Strong, C.P., Talarico, F., Verosub, K.L., Villa, G., Webb, P-N., Wonik, T., 2001. Orbitally induced oscillations in the East Antarctic Ice Sheet at the Oligocene/Miocene boundary. Nature 413, 719–723.

Naish, T., Powell, R., Levy, R., Wilson, G., Scherer, R., Talarico, F., Krissek, L., Niessen, F., Pompilio, M., Wilson, T., Carter, L., DeConto, R., Huybers, P., McKay, R., Pollard, D., Ross, J., Winter, D., Barrett, P., Browne, G., Cody, R., Cowan, E., Crampton, J., Dunbar, G., Dunbar, N., Florindo, F., Gebhardt, C., Graham, I., Hannah, M., Hansaraj, D., Harwood, D., Helling, D., Henrys, S., Hinnov, L., Kuhn, G., Kyle, P., Läufer, A., Maffioli, P., Magens, D., Mandernack, K., McIntosh, W., Millan, C., Morin, R., Ohneiser, C., Paulsen, T., Persico, D., Raine, I., Reed, J., Riesselman, C., Sagnotti, L., Schmitt, D., Sjunneskog, C., Strong, P., Taviani, M., Vogel, S., Wilch, T., Williams, T., 2009. Obliquity-paced Pliocene West Antarctic Ice Sheet oscillations. Nature 458, 322–328.

Orombelli, G., Baroni, C., Denton, G.H., 1990. Late Cenozoic glacial history of the Terra Nova Bay region, Northern Victoria Land, Antarctica. Geogr. Fis. Din. Quat. 13, 139–163.

Rignot, E., Mouginot, J., Scheuchl, B., 2011. Ice flow of the Antarctic ice sheet. Science 333, 1427–1430.

Rodés, A., Pallás, R., Braucher, R., Moreno, X., Masana, E., Bourlés, D.L., 2011. Effect of density uncertainties in cosmogenic ^{10}Be depth-profiles: Dating a cemented Pleistocene alluvial fan (Carboneras Fault, SE Iberia). Quat. Geochronol. 6 (2), 186–194. http://dx.doi.org/10.1016/j.quageo.2010.10.004.

Ross, N., Jordan, T.A., Bingham, R.G., Corr, H.F.J., Ferraccioli, F., Le Brocq, A.M., Rippin, D.M., Wright, A.P., Siegert, M.J., 2014. The Ellsworth subglacial highlands: inception and retreat of the West Antarctic ice sheet. Geol. Soc. Am. Bull. 126, 3–15.

Rutford, R.H., 1972. Glacial geomorphology of the Ellsworth Mountains. In: Adie, R.J. (Ed.), Antarctic Geology and Geophysics, Oslo, Universitetsforlaget, pp. 225–232.

Rutford, R.H., Denton, G.H., Andersen, B.G., 1980. Glacial history of the Ellsworth Mountains. Antarc. J. U.S. 15, 56–57.

Scherer, R.P., DeConto, R.M., Pollard, D., Alley, R.B., 2016. Windblown Pliocene diatoms and East Antarctic ice sheet retreat. Nat. Commun. 7, 12957. http://dx.doi.org/10.1038/ncomms12957. 9 pp.

Shevenell, A.E., Kennett, J.P., Lea, D.W., 2004. Middle Miocene Southern Ocean cooling and Antarctic cryosphere expansion. Science 305 (5691), 1766–1770.

Spörli, K.B., Craddock, C., 1992. Stratigraphy and structure of the Marble, Independence and Patriot Hills, Heritage Range, Ellsworth Mountains, West Antarctica. Geol. Soc. Amer. Mem. 170, 375–392.

Stern, T.A., Baxter, A.K., Barrett, P.J., 2005. Isostatic rebound due to glacial erosion within the Transantarctic Mountains. Geology 33, 221.

Storey, B.C., Dalziel, I.W.D., Garrett, S.W., Grunow, A.M., Pankhurst, R.J., Vennum, W.R., 1988. West Antarctica in Gondwanaland: crustal blocks,reconstruction and breakup processes. Tectonophysics 155, 381–390.

Sugden, D.E., Denton, G.H., 2004. Cenozoic landscape evolution of the Convoy Range to Mackay glacier area, Transantarctic Mountains: onshore to offshore synthesis. Geol. Soc. Am. Bull. 116, 840–857.

Sugden, D.E., Denton, G.H., Marchant, D.R., 1995. Landscape evolution of the Dry Valleys, Transantarctic Mountains; tectonic implications. J. Geophys. Res. 100 (B7), 9949–9967.

Sugden, D.E., Fogwill, C.J., Hein, A.S., Stuart, F.M., Kerr, A.R., Kubik, P.W., 2014. Emergence of the Shackleton Range from beneath the Antarctic ice sheet due to glacial erosion. Geomorphology 208, 190–199. http://dx.doi.org/10.1016/j/geomorph.2013.12.004.

Summerfield, M.A., 1991. Global Geomorphology. Longman, London.

Warny, S., Askin, R.A., Hannah, M.J., Mohr, B.A.R., Raine, J.I., Harwood, D.M., Florindo, F., SMS Science Team, 2009. Palynomorphs from a sediment core reveal a sudden remarkably warm Antarctica during the middle Miocene. Geology 37, 955–958. http://dx.doi.org/10.1130/G30139A.1.

Webers, G.F., Craddock, C., Splettstoesser, J.F., 1992. Geologic history of the Ellsworth Mountains, West Antarctica. Geol. Soc. Amer. Mem. 170, 1–8.

Westoby, M.J., Dunning, S.A., Woodward, J., Hein, A.S., Marrero, S.M., Winter, K., Sugden, D.E., 2016. Interannual surface evolution of an Antarctic blue-ice moraine using multi-temporal DEMs. Earth Surf. Dyn. 4, 515–529.

Winter, K., Woodward, J., Ross, N., Dunning, S.A., Bingham, R.G., Corr, H.F.J., Siegert, M.J., 2015. Airborne radar evidence for tributary flow switching in Institute ice stream, West Antarctica: implications for ice sheet configuration and dynamics. J. Geophys. Res., Earth Surf. 120.